Irreversible adsorption of particles at random-site surfaces

Zbigniew Adamczyk, Katarzyna Jaszczółt, Barbara Siwek, and Paweł Weroński

Citation: The Journal of Chemical Physics **120**, 11155 (2004); doi: 10.1063/1.1712967
View online: http://dx.doi.org/10.1063/1.1712967
View Table of Contents: http://scitation.aip.org/content/aip/journal/jcp/120/23?ver=pdfcov
Published by the AIP Publishing

Irreversible adsorption of particles at random-site surfaces

Zbigniew Adamczyk,[a] Katarzyna Jaszczółt, Barbara Siwek, and Paweł Weroński
Institute of Catalysis and Surface Chemistry, Polish Academy of Sciences, 30-239 Kraków, Niezapominajek 8, Poland

(Received 24 November 2003; accepted 1 March 2004)

Irreversible adsorption of negatively charged polystyrene latex particles (averaged diameter 0.9 μm) at heterogeneous surfaces was studied experimentally. The substrate bearing a controlled number of adsorption sites was produced by precovering mica sheets by positively charged polystyrene latex (averaged diameter of 0.45 μm). Positive latex (site) deposition was carried out under diffusion-controlled transport conditions and its coverage was determined by direct particle counting using the optical microscopy. Deposition kinetics of larger latex particles (averaged diameter 0.9 μm) at heterogeneous surfaces produced in this way was studied by direct optical microscope observations in the diffusion cell (under no-convection transport conditions). It was demonstrated that the structure of larger particle monolayers, characterized in terms of the pair correlation function, showed much more short-range ordering than it was predicted for homogeneous surface monolayers at the same coverage. This was found in agreement with theoretical predictions derived from the Monte Carlo simulations. On the other hand, particle adsorption kinetics was quantitatively interpreted in terms of numerical solutions of the governing diffusion equation with the nonlinear boundary condition derived from Monte Carlo simulations. From these kinetic measurements maximum (jamming) coverage of particles was determined in an accurate way by extrapolation. It was concluded that both the monolayer structure and jamming coverage were strongly influenced by the site multiplicity (coordination) effect.
[DOI: 10.1063/1.1712967]

I. INTRODUCTION

Adsorption and deposition (irreversible adsorption) of colloids, proteins and other biomaterials on solid/liquid interfaces is of large significance for many practical and natural processes such as filtration, papermaking, chromatography, separation of proteins, viruses, bacteria, pathological cells, immunological assays, thrombosis, biofouling, biomineralization, etc. The effectiveness of these processes is often enhanced by the use of coupling agents bound to interfaces, e.g., polyelectrolytes.[1–5] In biomedical applications special proteins (antibodies) attached to the surface are applied for a selective binding of a desired ligands from protein mixtures as is the case in the affinity chromatography,[6] recognition processes (biosensors),[7,8] immunological assays,[9,10] etc.

On the other hand, many of experimental studies on colloid particle adsorption have been carried out for surfaces modified by adsorption of polymers, surfactants, polyvalent ions, or chemical coupling agents (silanes), which change the natural surface charge of substrate surfaces.[11,12] Another important example is adsorption of ionic species, e.g., heavy metal ions, at oxide surfaces bearing various sites, usually characterized by a wide spectrum of binding energy.[13] As demonstrated in Refs. 14 and 15 ion adsorption often leads to nonuniform distribution of charges, e.g., over the glass beads used in the packed bed filtration processes. Appearance of such heterogeneous interfaces may exert important effects on transport of colloid particles in aqueous porous media, e.g., in soils.[16]

A characteristic feature of all these processes, also comprising chemisorption of gases on solids, is that the solute (ion, particle or protein) adsorption occurs at heterogeneous surfaces bearing isolated adsorption sites.

Despite significance of particle adsorption at heterogeneous surfaces, this subject has little been studied experimentally in a systematic manner. Most of the existing results have been obtained for colloid hematite particles[17,18] or polymeric latex particles[16,19] in the packed bed columns. Other measurements have been carried out for polystyrene latex particles of micrometer size range adsorbing at mica under the convection-dominated transport conditions.[20,21] To the best of our knowledge there are no experimental data reported in the literature for the diffusion-controlled transport, except for preliminary results presented in Ref. 22.

Therefore, the aim of this work was to perform systematic experiments of this type in a model system of latex particle adsorbing at mica surface bearing adsorption sites of a well defined geometry and distribution. Besides practical significance, these measurements will allow one to evaluate the range of validity of the recent theoretical model describing irreversible adsorption (deposition) of particles at heterogeneous surfaces.[23,24] Especially interesting would be evaluating the jamming coverage of particles in relation of the site density that is vital for many applications in medicine. Additionally, the results obtained can be exploited for elucidating mechanisms and modeling the kinetics of molecular ad-

[a]Author to whom correspondence should be addressed. Electronic mail: ncadamcz@cyf-kr.edu.pl

sorption processes as well, e.g., to determine the validity of the often used Langmuir model.

II. EXPERIMENT

A. The experimental cell

Particle deposition experiments have been carried out using the direct microscope observation method in the diffusion cell. The main part of the cell was a teflon container of dimensions $1.5\times 2.5\times 8$ cm (height) with an rectangular window of the dimension of 2×6 cm made of a mica sheet, used as the substrate for particle adsorption. Similar set-up was used previously in studies of particle adsorption at homogeneous surfaces.[25,26] The cell was fixed to the optical microscope stage (Nikon) that was attached to a special metal table, which could be inclined (rotated) by an angle reaching 90°. In the latter case, the microscope was oriented horizontally with the objective perpendicular to the substrate surface. In this arrangement gravity was directed parallel to the mica surface eliminating effectively the particle sedimentation effect. In order to eliminate the natural convection effects both the cell and the room have been thoroughly thermostated at 25 °C. Deposition kinetics and particle distribution over the substrate was followed *in situ* using the Nikon microscope equipped with a long-distance objective coupled with a CCD camera (Hamamatsu C-3077) and an image analyzing system.

B. Materials and methods

Two samples of polystyrene latex were used as model colloid systems in the present study of particle deposition. These latex particles of submicrometer size range are known to posses perfectly spherical shape and low polidispersity.[12] The negatively charged latex suspension was synthesized according to the polymerization procedure described in Ref. 27 using a persulfate initiator. The concentrated stock suspension obtained from the polymerization was purified by a steam distillation and a prolonged membrane filtration according to the procedure described previously.[11] Particle size distribution and concentration in the dilute samples used in experiments were determined by the Coulter–Counter and by laser diffractometer with an accuracy of a few percent. The averaged size $2a_p$ of the negative latex used in deposition experiments was 0.9 μm with a standard deviation of 0.06 μm. The positively charged latex suspension (used for modelling adsorption sites) was produced and cleaned according to a similar procedure with the azonitrile initiator in place of the persulfate initiator. The averaged diameter of the positive latex $2a_s$ was 0.45 μm with the standard deviation of 0.04 μm as determined by a laser diffractometer. Hence, the particle size ratio being an important parameter, denoted by λ, was equal to 2 in our case.

Zeta potential of latex samples was determined by the Brookhaven zetasizer. For the ionic strength I of 10^{-3} M, adjusted by KCl addition, and $p\mathrm{H}=5.5$ prevailing in experiments, zeta potential of the negative latex was -52 mV, whereas for the positive latex it was 50 mV, respectively.

The adsorbing (substrate) surfaces were prepared of mica sheets provided by Mica and Micanite Supplies Ltd., England. Zeta potential of this mica was determined by the streaming potential method in the plane-parallel channel cell.[28] For the above experimental conditions the zeta potential on mica was -80 mV.

The experimental procedure was the following: A freshly cleaved mica sheet was cut to the appropriate size and mounted into the cell's window without using any adhesive. Then, the positive latex suspension was carefully poured into the cell. Particle deposition was carried out for a desired time (typically 15–60 min at bulk particle concentration changing in the range of 10^9-10^{10} cm^{-3}) until the prescribed surface concentration of the particles was attained. The surface concentration was determined by a direct microscope counting over statistically chosen areas. The total number of particles counted was about 1000 that ensured a relative precision of coverage determination better than 3%. For the sake of convenience the surface concentration of particles was expressed as the dimensionless coverage $\Theta_s=\pi a_s^2\langle N_s\rangle$ (where $\langle N_s\rangle$ is the average surface concentration of adsorbed smaller particles). In our experiments Θ_s varied between 0 and 0.25. After preparing the heterogeneous substrate (mica covered by adsorption sites) the positive latex suspension was replaced by 10^{-3} M KCl solution and then by the negative latex suspension and the particle deposition run was continued for a period reaching 50 hs. The bulk suspension concentration of the negative latex n_b was typically $2-5\times 10^9$ cm^{-3} in these experiments. Images of adsorbed particles were collected *in situ* at prescribed time intervals. Adsorption kinetics of latex was followed by determining the averaged surface concentration $\langle N_p\rangle$ of particles found on these images as a function of the time t. For obtaining a single point on the kinetic curve, 500–1000 particles were counted over statistically chosen areas having typical dimensions of 100 per 100 μm. The dimensionless surface coverage of adsorbed larger particles was expressed as $\Theta_p=\pi a_p^2\langle N_p\rangle$. After completing the deposition run the latex suspension was carefully washed out by water and the mica surface covered with particles was examined again under wet conditions. This procedure was selected because it has been observed that drying up of the sample induced significant structure changes in the particle monolayer.

It also was proven in separate experiments that particle adsorption of both lattices was perfectly irreversible and localized. No lateral motion or particle desorption was observed when rinsing *in situ* particle monolayers with an electrolyte, 10^{-3} KCl, by a prolonged period of time.

III. RESULTS AND DISCUSSION

Because of the relatively large size of both negative and positive latex particles used in our experiments, they could be observed under optical microscope that allowed one to determine not only surface concentration but also relative positions (coordinates) of particles. Moreover, due to larger size ratio, both the uncovered sites and adsorbed particles could be easily discern from each other that considerably enhanced the reliability of the experimental data discussed below.

In the first series of experiments, the kinetics of positive

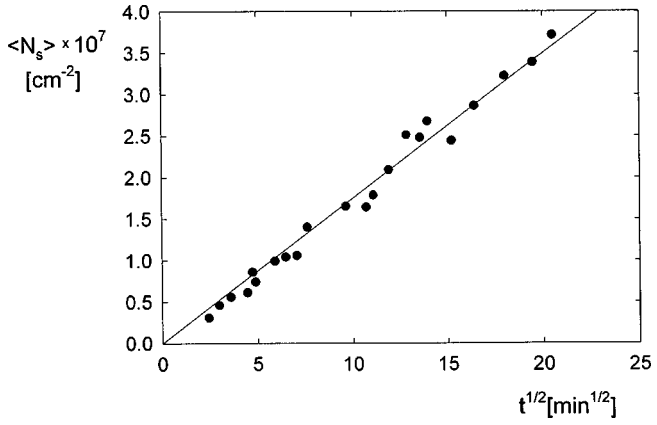

FIG. 1. Initial adsorption kinetics of positive latex (averaged diameter 0.45 μm) at bare mica, $I=10^{-3}$ M, $n_b=2.0\times10^9$ cm^{-3} (points), the solid line denotes theoretical results calculated from Eq. (1).

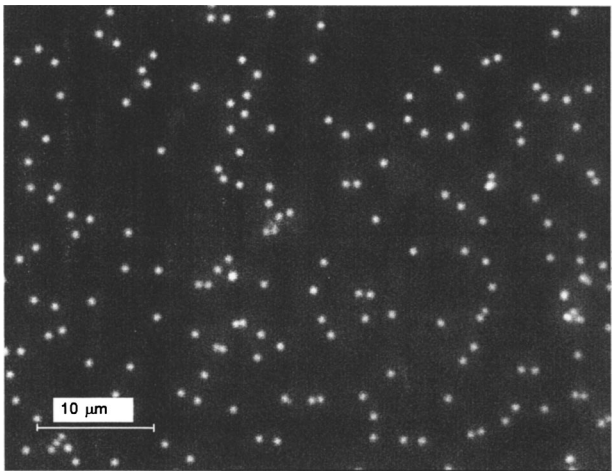

FIG. 2. A micrograph of sites (positive latex particles adsorbed on mica), $\Theta_s=0.014$.

latex adsorption was quantitatively evaluated in order to select appropriate conditions for controlled preparation of substrate surfaces bearing a desired coverage of sites. A typical kinetic run observed for bulk suspension concentration $n_b=2\times10^9$ cm^{-3} is shown in Fig. 1. As can be observed, the surface concentration of sites $\langle N_s\rangle$ (consequently the site coverage Θ_s) increased linearly with the square root of the deposition time t, in accordance with diffusion-controlled transport to a plane surface, described by the formula

$$\langle N_s\rangle=2\sqrt{\frac{D_s t}{\pi}}n_b, \tag{1}$$

where $D_s=kT/6\pi\eta a_s$ is the diffusion coefficient of the particle in the bulk (k is the Boltzmann constant, T is the absolute temperature, and η is the dynamic viscosity of the suspension). Because both $\langle N_s\rangle$ (the averaged number of particles per unit area) and n_b can be determined experimentally (the latter quantity via the direct dry weight method), one can use Eq. (1) to calculate the diffusion coefficient of particles. In this way, by knowing the temperature and the viscosity of the suspension one can determine particle size. From the kinetic run shown in Fig. 1 it was found in this way that $2a_s=0.47$ μm that is in a good agreement with the value obtained from the diffractometer.

Equation (1) was also used for predicting the adsorption time needed to attain a desired surface concentration (coverage) of sites. However, the real coverage in every run was determined, as mentioned above, by a direct counting of the number of adsorbed particles.

Besides the coverage, the uniformity of site distributions produced according to the above procedure has been examined. First, it was demonstrated by a throughout variance analysis (carried out for various areas over the mica substrate covered by sites) that latex particle distributions were statistically uniform with no tendency to clustering as is often the case for monolayers dried before microscope observation. This can be qualitatively observed in Fig. 2, where a micrograph of sites is shown for $\Theta_s=0.014$. However, because of small particle size, comparable with the visible light wavelength, a quantitative characteristic of site distribution in terms of the pair correlation function was not feasible.

After establishing the conditions for producing well-defined site distributions of desired coverage, systematic studies of larger particles deposition has been performed with the aim of determining the structure of particle monolayers and kinetic of their formation. Examples of large particle configurations obtained in these experiments are shown in Figs. 3 and 4. In Fig. 3 the limiting case of low site coverage $\Theta_s=0.014$ is presented for particle coverage Θ_p equal to 0.044 and 0.075.

As can be estimated, the average distance between sites $\sqrt{\pi a_s^2/\Theta_s}$ was equal $15.0a_s$ for $\Theta_s=0.014$ that considerably exceeded the site and particle dimensions. This estimation indicates that the sites can be largely treated as isolated targets because particles adsorbed on various sites will not interfere with each other. This phenomenon can indeed be observed in the micrograph shown in Fig. 3. It is seen that the adsorbed particles are very unevenly distributed with tendency to form assemblages, usually composed of two or three particles attached to one site. Remembering that particles have been observed under wet conditions that eliminated possible clustering via drying, one can assume that these assemblages have been really produced in the deposition process. This interesting observation represents apparently the first evidence of the site multiplicity effect occurring in the colloid adsorption processes. From simple geometry one can deduce that site multiplicity effect (simultaneous attachment of more than one particle to one adsorption site) may only appear for particle to site size ratio $\lambda<4$. On the other hand, in our case, for $\lambda=2$, there could be maximum four particles attached to one site that qualitatively explains the appearance of particle clusters.

Due to larger particle size, the distributions shown in Fig. 3 can be quantitatively evaluated in terms of the pair correlation function $g(r)$ (referred often to as the radial distribution function). The function was calculated from the constitutive dependence

$$g(r)=\frac{\pi a_p^2}{\Theta_p}\left\langle\frac{\Delta N_p}{2\pi r\Delta r}\right\rangle, \tag{2}$$

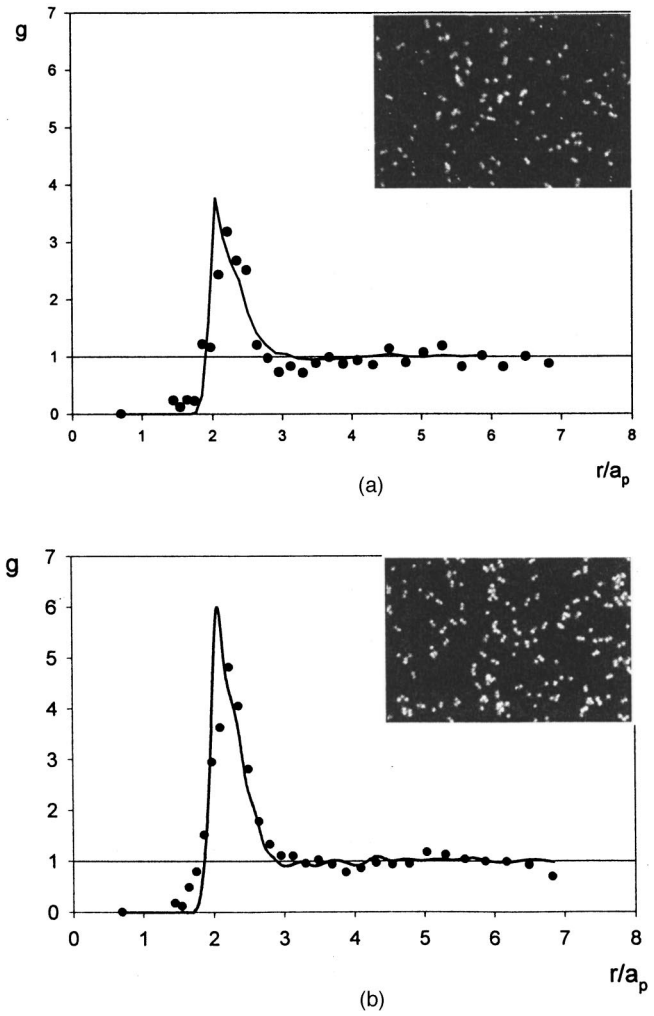

FIG. 3. Micrographs of negative latex particles (averaged diameter 0.9 μm) adsorbed on sites, $\Theta_s=0.014$, and the corresponding pair correlation function $g\ (r/a_p)$. (a) $\Theta_p=0.044$; (b) $\Theta_p=0.075$. The solid lines denote the theoretical pair correlation function derived from the extended RSA model.

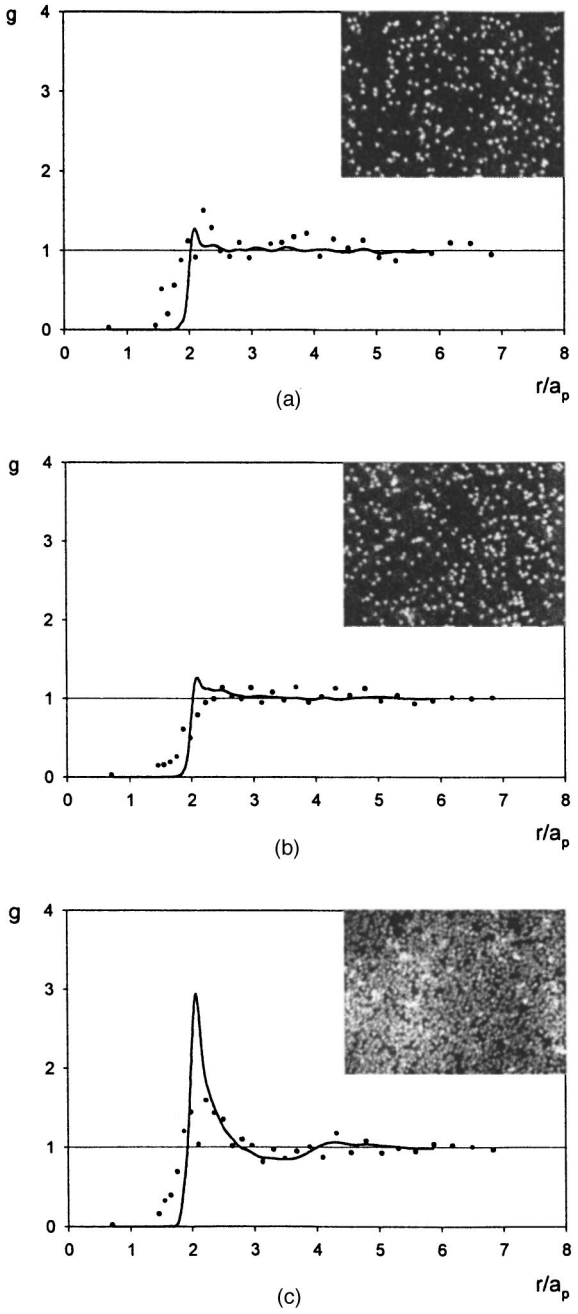

FIG. 4. Same as for Fig. 3 but for site coverage $\Theta_s=0.104$. (a) $\Theta_p=0.047$; (b) $\Theta_p=0.095$; (c) $\Theta_p=0.486$. The solid lines denote the theoretical pair correlation function derived from the extended RSA model.

where $\langle\ \rangle$ means the ensemble average and N_p is the number of particles adsorbed within the ring $2\pi r\ \Delta r$ drawn around a central particle. The function can be interpreted as an averaged probability of finding a particle at the distance r from another particle (with the center located at $r=0$) normalized to the uniform probability at large distances. For sake of convenience the distance r was normalized by using the particle radius a_p as a scaling variable.

The $g(r/a_p)$ function plotted in Fig. 3 was evaluated using Eq. (2) by analyzing coordinates of a few thousands of particles according to the procedure described above. However, it should be remembered, that in this case the distance r was measured between projections of particle centers onto the adsorption plane, rather than between particle centers themselves. A characteristic feature of the $g(r/a_p)$ function shown in Fig. 3 is that it exhibits a well pronounced maximum at the distance $r/a_p=2$ whose height increased monotonically with particle coverage Θ_p. Another interesting fact is that this function was not vanishing for the distance $r/a_p<2$ but rather at $r_{\min}/a_p$ of about$=1.7$. The non vanishing value of g observed for this distance range spectacularly confirmed the fact that particles were adsorbed in various planes as a result of the finite size of the adsorption sites. This means that their projections on the adsorption plane could overlap. This apparent overlapping effect is analogous to previously observed for adsorption at homogeneous interfaces of polydisperse particles.[29] It is interesting to compare the experimentally found minimum distance $r_{\min}$ with the value predicted theoretically for particle size ratio occurring in our experiments. This can be done by realizing that the minimum distance between projection of particle centers appears when one particle touches the substrate surface and simultaneously another particle (and obviously the site). Moreover, the centers of the two particles and the site lie in one plane perpendicular to the substrate surface. From a simple geometry one

can deduce then that the distance $r_{\min}$ is given by the expression

$$r_{\min}/a_p = 2[2a_p\sqrt{a_p a_s} + (a_p - a_s)\sqrt{a_s(2a_p + a_s)}]/(a_p + a_s)^2$$
$$= 2[2\lambda\sqrt{\lambda} + (\lambda - 1)\sqrt{2\lambda + 1}]/(1 + \lambda)^2, \quad (3)$$

where, as mentioned above, $\lambda = a_p/a_s$.

One can predict from Eq. (3) that for our geometry, when $\lambda = 2$, $r_{\min}/a_p = 1.75$ that agrees well with the value found experimentally (see Fig. 3). Interestingly enough, one can calculate from Eq. (3) that for $\lambda = 4$, $r_{\min}/a_p = 2$, that agrees with previous conclusion that $\lambda = 4$ is the limiting value when two particles can be attached to one site.

On the other hand, from geometrical considerations one also can predict the maximum distance r_{mx} between two particles attached to one site and contacting the substrate surface as well that is given by the simple formula valid for $\lambda < 4$,

$$r_{\mathrm{mx}}/a_p = 4/\sqrt{\lambda}. \quad (4)$$

As can be deduced, in our case $r_{\mathrm{mx}}/a_p = 4/\sqrt{2} = 2.83$. One can expect that for distances larger than r_{mx} the pair correlation function g should approach unity since adsorbed particle positions remain uncorrelated (particles adsorbed on various sites do not interfere with each other as mentioned above). Indeed, one can observe in Figs. 3 and 4, that g approaches unity for $r/a_p > 2.8$.

It is interesting to observe that all the characteristic features of the correlation function shown in Fig. 3 are well reflected by theoretical predictions depicted by solid lines. These theoretical results have been derived from Monte Carlo simulations performed according the theoretical model described in Refs. 23 and 24. The first step of the simulation algorithm was covering the homogeneous interface by adsorption according to the classical random sequential adsorption (RSA) approach.[30–35] The basic feature of this model is that particles are placed at random in a consecutive manner over an adsorption plane of isotropic properties. If there is no overlapping with previously adsorbed particle the incoming (virtual) particle is adsorbed irreversibly at a given position with unit probability. Otherwise, a new adsorption attempt is repeated, uncorrelated with previous attempts. The process is carried out until a prescribed coverage of particles is attained. It was postulated in Ref. 35 that particle configurations produced under the diffusion transport conditions are better reflected by the diffusion RSA (DRSA) model that considers to some extent correlations in the consecutive adsorption attempts. The pair correlation function in this case exhibits a higher maximum for transient coverage of sites, than the classical RSA model. Since these differences are too small to be detected experimentally and the simulation algorithm is far more complicated than the classical RSA model, we exploited the latter for producing site distributions of desired coverage.

The second step of simulations was adsorption of particles on site covered surfaces that was done by sequentially performing uncorrelated adsorption attempts of a virtual particle. The attempt was successful if the virtual particle touched at least one site and simultaneously did not overlap with any previously adsorbed particle. It was further assumed that the coordinates of particles remained fixed during the entire simulation run that implies a localized and irreversible adsorption. In this respect our calculation scheme was similar to that used for RSA simulations of multilayer deposition of particles.[34,36–39]

A good agreement of experimental and simulation data with the analytical estimations derived from Eqs. (3) and (4) indicates that by analysing the shape of the pair correlation function (especially the $r_{\min}$ and r_{mx} values) important clues can be gained about the size and coverage of sites present at a substrate. Obviously, this possibility is especially attractive for sites of unknown size, invisible under an optical microscope.

In Fig. 4 analogous results obtained for much higher site coverage Θ_s are presented. The averaged distance between sites was in this case 5.6 a_s that implied a considerable interference of particles adsorbed at various sites reducing the appearance of the site multiplicity effect. Indeed, it can be seen in the micrographs presented in Fig. 4 that the particles are more evenly distributed than previously that is reflected by much lower maximum of the pair correlation function for lower particle coverage range. The maximum increases for the high coverage of particles $\Theta_p = 0.48$, close to the jamming limit. Note, however, that the value of experimentally determined value of $r_{\min}$ remains very similar to the previously studied case of low Θ_s. It is also interesting to observe that the experimental results shown in Fig. 4 are well reflected by the numerical simulations.

Besides studying the structural aspects discussed above, the main goal of this work was to confirm experimentally the validity of the theoretical predictions concerning the jamming limit dependence on site coverage. This is vital in view of the practical significance of this parameter. However, as discussed in previous works on diffusion controlled adsorption of colloid particles, direct measurement of the jamming coverage are very tedious with typical times of a single experiment reaching 50 h. Therefore, it was suggested that the most efficient procedure of determining Θ_p consist in performing the entire kinetic run, i.e., the dependence of Θ_p on adsorption time within a finite time interval and extrapolate them to infinite time by using theoretical models formulated in Ref. 40. This significantly increases the precision of jamming coverage determination.

Typical kinetic runs evaluated for various site coverage Θ_s ranging from 0.016 to 0.22 are presented in Fig. 5. In order to facilitate the comparison with the limiting diffusion transport law the results have been presented in the form of the dependence of Θ_p on the square root of adsorption time $t^{1/2}$. As can be seen in Fig. 5 for $\Theta_s > 0.05$ and $\Theta_p < 0.1$ the initial adsorption kinetics of particles was indeed linear when expressed in this coordinate system. This means that particle coverage is well reflected by Eq. (1), written as

$$\langle N_p \rangle = 2\sqrt{\frac{D_p t}{\pi}}\, n_b, \quad (5)$$

where D_p is the particle diffusion coefficient and n_b is the particle number concentration in the bulk.

This means that for site coverage as low as a few percent, particle adsorption rate at heterogeneous surfaces at-

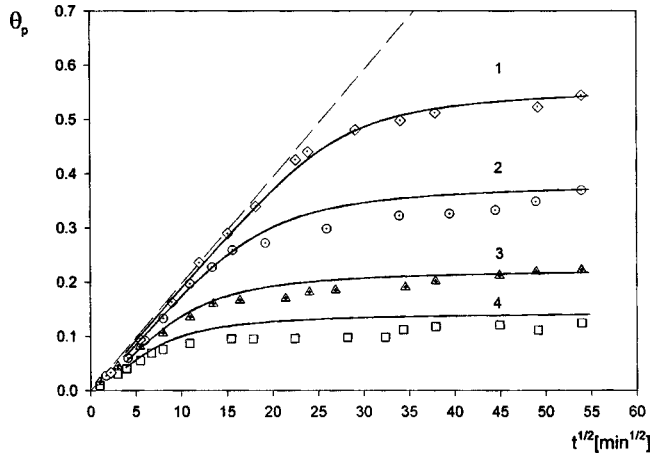

FIG. 5. Adsorption kinetics of negative latex at heterogeneous surfaces for the nonlinear regime expressed as the Θ_p vs $t^{1/2}$ dependence, $n_b=4.8\times10^9$ cm^{-3}. (1) $\Theta_s=0.224$; (2) $\Theta_s=0.058$; (3) $\Theta_s=0.027$; (4) $\Theta_s=0.016$. The solid lines denote the theoretical results calculated numerically by solving numerically the diffusion equation with the boundary condition, the dashed line represents the theoretical results calculated from Eq. (5) in the case of no blocking.

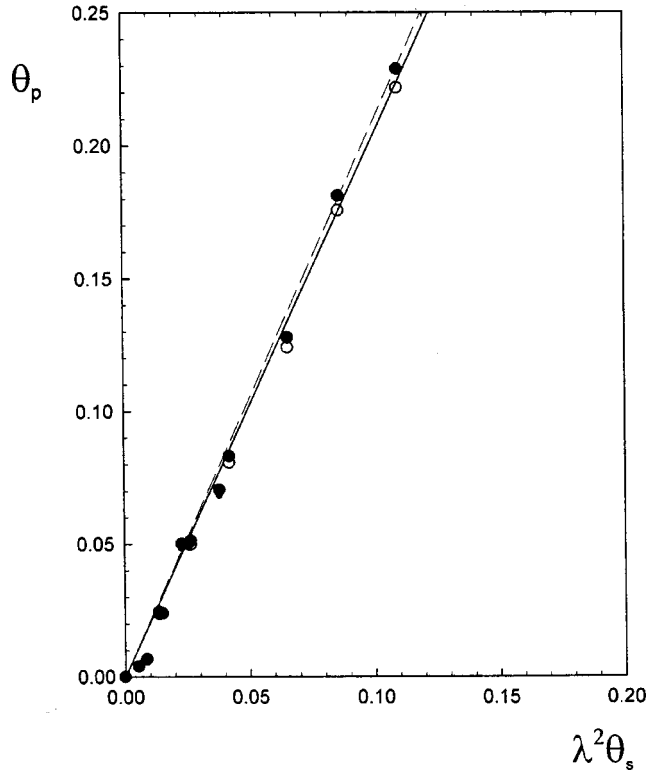

FIG. 6. The maximum (jamming) coverage of particles Θ_p as a function of $\lambda^2\Theta_s$. Full symbols denote the experimental data extrapolated via Eq. (6), the empty symbols show the unextrapolated experimental data fitted by the straight-line dependence (solid line), the dashed line represents the theoretical Monte Carlo simulations (smoothened).

tained the limiting value pertinent to uniform surfaces under the diffusion-controlled transport conditions. This unexpected behavior can be interpreted physically, as suggested in Refs. 20–21, as due to the fact that after a failed adsorption attempt a particle can reach by diffusion another adsorption site in their vicinity, before it returns to the bulk of the suspension. This means that for this coverage range the overall transport rate is governed by the diffusion transport in the bulk of the suspension rather than by the surface transport step whose rate is determined by site coverage. The effects connected with the surface transport start to play a more significant role for very low site coverage or for high particle coverage approaching the jamming limit.[21,22] Indeed, it can be observed in Fig. 5, that for higher particle coverage a significant deviation of adsorption kinetics from linearity (expressed in terms of the square root of adsorption time) occurred as a results of increased surface blocking effects studied extensively for uniform surface adsorption.[12,26,29] As a result particle adsorption rate decreased gradually with the adsorption time and particle coverage attained apparent saturation values.

A quantitative interpretation of these effects can be performed in terms of the theoretical model developed in Refs. 22, 40. According to this approach, the kinetics of particle adsorption at heterogeneous surfaces can be evaluated by formulating a nonlinear boundary condition for the diffusion transport equation incorporating the initial adsorption probability and the available surface function. Both these quantities have been determined from the Monte Carlo simulations performed according to the above described algorithm. The diffusion equation with this boundary condition can be solved by using the implicit finite-difference method as described in detail elsewhere.[40] As can be seen in Fig. 5, our experimental data obtained for various Θ_s, are well reflected by these theoretical calculations (depicted by continuous lines) for the entire range of adsorption time studied, reaching 50 h. It is worthwhile noting that no adjustable parameters have been used by evaluating the theoretical data shown in Fig. 5 but merely the experimental value of the particle size ratio λ and the site coverage Θ_s. It should be remembered, however, that in due to the finite adsorption time the saturation values of particle coverage as shown in Fig. 5 are slightly lower than the true jamming limit. As mentioned, the jamming coverage can be estimated by extrapolation of the experimental data obtained for long times using the procedure proposed in Ref. 40. The following analytical expression has been derived, whose validity was confirmed by extensive numerical calculations:

$$\Theta_p^{\infty}=\Theta_l\left[1+0.372\sqrt{\frac{\Theta_l}{\xi D_p a_p n_b t_l}}\right], \tag{6}$$

where Θ_l is the particle coverage determined experimentally for the maximum adsorption time t_l, and ξ is the dimensionless parameter of the order of 0.1 characterizing the surface transport resistance.[40] Inserting our experimental data into Eq. (6), i.e., $D_p=4.8\times10^{-9}$ cm^2/s, $n_b=4.8\times10^9$ cm^{-3}, $t_l=1.8\times10^5$ s one can estimate that the correction varies between 0.5% for $\Theta_l<0.2$ and 1% for $\Theta_l>0.3$. Hence, for $\Theta_l<0.1$, the correction is well below the experimental error, so the experimental and theoretical data should be statistically indistinguishable.

Indeed, the results plotted in Fig. 6 using the Θ_p vs $\lambda^2\Theta_s$ coordinate system confirm this hypothesis. This kind of representation of the experimental results is advantageous because according to theoretical predictions[24] the depen-

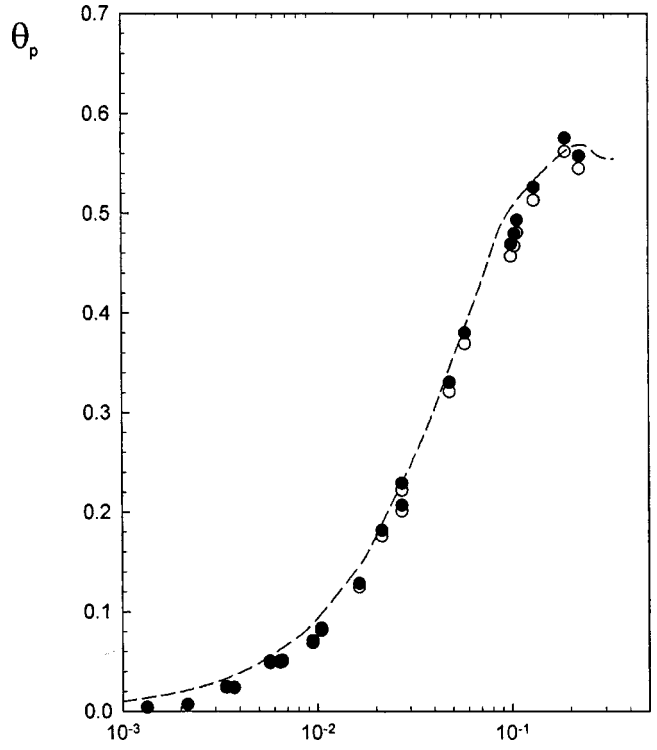

FIG. 7. The maximum (jamming) coverage of particles Θ_p as a function of site coverage Θ_s. Full symbols denote the extrapolated data, the empty symbols denote the unextrapolated experimental data, and the dashed line represents the theoretical Monte Carlo simulations (smoothened).

dence of Θ_p on $\lambda^2\Theta_s$ in the limit of low site coverage should be linear with the slope equal to the site multiplicity (coordination number), denoted by n_s. As can be seen in Fig. 6 the experimental data can indeed be fitted by a straight line dependence having the slope of 2.04. This agrees well with the averaged value of n_s, derived from simulations, equal to 2.09 for $0<\lambda^2\theta_s<0.1$. One can conclude, therefore, that the appearance of the site multiplicity effect, suggested previously by the large maximum of the pair correlation function (see Fig. 3), is spectacularly confirmed by these data.

It should be mentioned, however, that in the limit of $\lambda^2\theta_s\rightarrow 0$ the theoretical value of n_s approached 2.45, as determined from simulations. This difference (in comparison with the previous value of 2.09) appears because with decreasing θ_s one adsorbing particle has a decreased chance of touching two sites simultaneously. Unfortunately, the experimental data for this very small range of site coverage are not accurate enough to confirm this effect.

This value of n_s (averaged number of particles adsorbed on site) can be qualitatively interpreted in terms of the geometrical model discussed previously. For low site coverage in the jamming state, one site can be blocked by one, two, three or maximum four particles. However, the one and four particle attachment event is highly improbable, so most of the sites bear two or there particles, as can be observed in Fig. 3. Assuming equal probability of these two configurations one obtains $n_s=2.5$ that is quite close to the theoretical and experimental value.

The accuracy of experimental data increases for higher site coverage range as can be seen in Fig. 7. A characteristic feature of the data is that the maximum coverage of particles is attained for θ_s as low as 0.1. This finding has a profound practical implications suggesting an efficient method for detecting the presence of surface heterogeneities (nanoparticles) on surfaces by adsorption of larger colloid particles. It is also worthwhile noting that the experimental data (extrapolated) exceed for higher site coverage the limiting value of 0.547 that was predicted theoretically for homogeneous surfaces.[31–34] This is in a good agreement with the present theoretical model (see the dashed line in Fig. 7) that predicts a maximum value of θ_p equal to 0.565 for $\theta_s=0.22$. A physical interpretation of the maximum is that for increasing site coverage, the surface area of sites available for particles becomes larger than the geometrical area of the interface because particles are adsorbed in different planes (quasi-3D). By increasing the site coverage, however, the average distance between sites becomes smaller than particle diameter, so a significant part of their surface area becomes inaccessible for particles. This effect is expected to reduce the available area for particles and consequently the jamming coverage.

It can be seen in Fig. 7, however, that for higher site coverage range some of the experimental data (extrapolated) deviate systematically from numerical simulations. This relative deviation is of the order of 3%. As demonstrated previously for homogeneous surface adsorption[26,41] this can be most probably attributed to the residual electrostatic repulsion among adsorbed particles. This is a plausible explanation because in our case, at the ionic strength of 10^{-3} M the thickness of the electric double layer was about 2% of adsorbing particle radius. As a result, the particles could not be treated as perfectly rigid spheres, that was the main assumption when performing numerical simulations. In accordance with theoretical estimations presented elsewhere,[12,26,41] the correction to the jamming coverage resulting from electrostatic repulsion is of the order of twice the double layer thickness, i.e., 4% in our case. This agrees with the value found in our experiments. It is worth mentioning, that corrections of this order of magnitude is not too significant from practical viewpoint.

IV. CONCLUSIONS

It was demonstrated experimentally that initial adsorption rates increased abruptly with the site coverage attaining the limiting value pertinent to uniform surfaces for Θ_s as small as a few percent. This was attributed to the fact that the overall transport was controlled by bulk diffusion of particles rather than by the surface transport resistance.

For higher coverage, particle adsorption kinetics deviated from linearity as a result of blocking effects. This effect was quantitatively accounted for by the theoretical approach based on numerical solutions of the diffusion equation with the nonlinear boundary conditions derived from simulations. The extrapolation of the kinetic runs allowed one to determine accurately the jamming coverage Θ_p as a function of the site coverage Θ_s. The experimental data were found in a good agreement with numerical simulations confirming an abrupt increase in the jamming coverage of particle with site coverage and presence of a maximum on the Θ_p vs Θ_s

curve. These findings, apparently the first of this kind in the literature, have been explained in terms of the site multiplicity effect and quasi-3D adsorption of particles. It also was shown that these effects influenced significantly the structure of adsorbed particle layers. A method of evaluating quantitatively the site multiplicity effect, was proposed.

It was suggested that the results obtained for model colloid particles can be exploited as useful reference states for predicting kinetics of protein and bioparticle adsorption at heterogeneous surfaces.

ACKNOWLEDGMENT

This work was supported by the KBN Grant No. 4T09A 076 25 and the EC Grant No. GRD1-2000-26823.

[1] M. Y. Boluk and T. G. M. van de Ven, Colloids Surf. **46**, 157 (1990).
[2] Y. Lvov, K. Ariga, I. Ichinose, and T. Kunitake, J. Am. Chem. Soc. **117**, 6120 (1995).
[3] T. Serizawa, H. Takashita, and M. Akashi, Langmuir **14**, 4088 (1998).
[4] J. Schmitt, P. Machtle, D. Eck, H. Mohwald, and C. A. Helm, Langmuir **15**, 3256 (1999).
[5] K. M. Chen, X. Jiang, L. C. Kimmerling, and P. T. Hammond, Langmuir **16**, 7825 (2000).
[6] H. A. Chase, Chem. Eng. Sci. **39**, 1099 (1984).
[7] I. Willner, M. Lion-Dagan, S. Marx-Tibbon, and E. Katz, J. Am. Chem. Soc. **117**, 6581 (1995).
[8] E. Katz, A. E. Buckmann, and I. Willner, J. Am. Chem. Soc. **123**, 10752 (2001).
[9] H. D. Inerowicz, S. Howell, F. E. Reniger, and R. Reifenberger, Langmuir **18**, 2563 (2002).
[10] S. W. Howell, H. D. Inerowicz, and R. Reifenberger, Langmuir **19**, 436 (2003).
[11] Z. Adamczyk, M. Zembala, B. Siwek, and J. Czarnecki, J. Colloid Interface Sci. **110**, 188 (1986).
[12] Z. Adamczyk, B. Siwek, M. Zembala, and P. Belouschek, Adv. Colloid Interface Sci. **48**, 151 (1994).
[13] W. Rudziński, R. Charmas, S. Partyka, F. Thomas, and J. Y. Bottero, Langmuir **8**, 1154 (1992).
[14] M. Elimelech and C. R. O'Melia, Langmuir **6**, 1153 (1990).
[15] L. Song and M. Elimelech, J. Colloid Interface Sci. **167**, 301 (1994).
[16] P. R. Johnson, N. Sun, and M. Elimelech, Environ. Sci. Technol. **30**, 3284 (1996).
[17] N. Ryde, H. Kihara, and E. Matijevic, J. Colloid Interface Sci. **151**, 421 (1992).
[18] A. Zelenev, V. Privman, and E. Matijevic, Colloids Surf. **135**, 1 (1998).
[19] P. R. Johnson, N. Sun, and M. Elimelech, Langmuir **11**, 801 (1995).
[20] Z. Adamczyk, B. Siwek, and E. Musiał, Langmuir **17**, 4529 (2001).
[21] Z. Adamczyk, B. Siwek, P. Weroński, and E. Musiał, Appl. Surf. Sci. **196**, 250 (2002).
[22] Z. Adamczyk, B. Siwek, P. Weroński, and K. Jaszczółt, Colloids Surf., A **222**, 15 (2003).
[23] Z. Adamczyk, P. Weroński, and E. Musiał, J. Chem. Phys. **116**, 4665 (2002).
[24] Z. Adamczyk, P. Weroński, and E. Musiał, J. Colloid Interface Sci. **248**, 67 (2002).
[25] Z. Adamczyk, L. Szyk-Warszyńska, B. Siwek, and P. Weroński, J. Chem. Phys. **113**, 11336 (2000).
[26] Z. Adamczyk and L. Szyk, Langmuir **16**, 5730 (2000).
[27] J. W. Goodwin, J. Hearn, C. C. Ho. C., R. H. Ottewill, Colloid Polym. Sci. **252**, 464 (1974).
[28] M. Zembala and Z. Adamczyk, Langmuir **16**, 1593 (2000).
[29] Z. Adamczyk, B. Siwek, M. Zembala, and P. Weroński, J. Colloid Interface Sci. **185**, 236 (1997).
[30] B. Widom, J. Chem. Phys. **44**, 3888 (1966).
[31] E. L. Hinrichsen, J. Feder, and T. Jossang, Langmuir **44**, 793 (1986).
[32] P. Schaaf and J. Talbot, J. Chem. Phys. **91**, 4401 (1989).
[33] J. W. Evans, Rev. Mod. Phys. **65**, 1281 (1993).
[34] J. Talbot, G. Tarjus, P. R. Van Tassel, and P. Viot, Colloids Surf., A **165**, 287 (2000).
[35] B. Senger, P. Schaaf, J. C. Voegel, A. Johner, A. Schmitt, and J. Talbot, J. Chem. Phys. **97**, 3813 (2000).
[36] V. Privman, H. L. Frisch, N. Ryde, and E. Matijevic, J. Chem. Soc., Faraday Trans. **87**, 1371 (1991).
[37] B. D. Lubachevsky, V. Privman, and S. C. Roy, Phys. Rev. E **47**, 48 (1993).
[38] B. D. Lubachevsky, V. Privman, and S. C. Roy, J. Comput. Phys. **126**, 152 (1993).
[39] V. Privman, Colloids Surf. A **165**, 231 (2000).
[40] Z. Adamczyk, J. Colloid Interface Sci. **229**, 477 (2000).
[41] Z. Adamczyk, *Irreversible Adsorption of Particles*, Chap. 5 in *Adsorption: Theory, Modeling and Analysis*, edited by J. Toth (Marcel-Dekker, New York, 2002), pp. 251–374.